KARYA ILHAM PUBLISHING
CONNECTING MINDS, BRIDGING IDEAS, INSPIRING READERS

Journal of Ship and Marine Structures

Journal homepage:
https://karyailham.com.my/index.php/jsms/index
ISSN: 3036-0137

Computational Prediction of a Propeller's Performance in Open Water Condition

Ahmad Fitriadhy[1,*], Nur Amira Adam[2], Kong Wai Sheng[3]

[1] Program of Naval Architecture, Faculty of Ocean Engineering Technology and Informatics, Universiti Malaysia Terengganu, Kuala Terengganu, Terengganu, Malaysia
[2] School of Port, Logistics and Management, Netherlands Maritime University College, Johor, Malaysia
[3] Program of Maritime Technology, Faculty of Ocean Engineering Technology and Informatics, Universiti Malaysia Terengganu, Kuala Terengganu, Terengganu, Malaysia

ARTICLE INFO

Article history:
Received 28 June 2023
Received in revised form 27 July 2023
Accepted 20 August 2023
Available online 25 September 2023

Keywords:
Propeller; CFD; blade number; RPM; pitch ratio; advance ratio

ABSTRACT

The marine propeller's performance is pivotal in overall ship design, ensuring efficient propulsion and desired speed. However, assessing propeller efficiency encounters limitations with empirical formulas and experiments. To accurately predict their performances during the initial design phase, a reliable investigation should be thoroughly carried out. The paper presents a computational analysis of the ship's propeller in open water conditions; whilst the hydrodynamic characteristics underlying the findings were comprehensively elucidated in the results. Several parameters such as the effect of rotational speed (RPM), blade number (Z), and pitch ratio (P/D) on thrust coefficient (K_T), torque coefficient (K_Q), and efficiency (η) have been accordingly taken into account. The results showed an inverse relationship between K_T and K_Q with the advance ratio (J), while efficiency increased at lower J values and decreased significantly at higher J values. The propellers with RPM of 1100 and Z=3 at J=0.8, and P/D=1.2 at J=1.0 exhibited the highest efficiencies of 76%, 69%, and 86%, respectively. A blade with a higher pitch ratio had a larger green region, indicating a lower-pressure region on the pressure side. These results contribute valuable insights to enhance marine propeller design and improve vessel fuel efficiency.

1. Introduction

The propeller, an important component in maritime propulsion, serves as a rotating fan-like structure designed to propel a ship through water efficiently. Its blades are meticulously shaped to generate pressure differences, thereby propelling the vessel forward. The size, shape, and number of blades are intricately designed to achieve optimal performance tailored to specific applications. The fundamental function of a propeller lies in its ability to convert rotational energy into thrust, playing an essential role in the overall efficiency and maneuverability of vessels. As advancements in

* *Corresponding author.*
E-mail address: naoe.afit@gmail.com

https://doi.org/10.37934/jsms.2.1.112b

engineering and design continue to evolve, the optimization of propeller characteristics becomes paramount for enhancing maritime transport and ensuring the effectiveness of propulsion systems.

To assess the efficiency of a propeller, various methods have been employed, including theoretical and experimental approaches. Utilizing empirical formulas, as done by Ekinci [1] and Tsujimoto *et al.,* [2], has limitations, particularly in neglecting dynamic interactions and relying on assumptions, especially in extreme conditions. Additionally, studies conducted through experiments may yield favorable results but may pose challenges in terms of simplifying the analysis. Some analyses may have proven difficult to visualize through figures, as demonstrated by Zou *et al.,* [3] and Ebrahimi *et al.,* [4]. To address these challenges, Computational Fluid Dynamics (CFD) has emerged as a viable alternative, offering a cost-effective and timely option for early design stages. Visualization aids in identifying flow patterns, and CFD results can validate experimental data, ensuring accuracy.

This paper investigates the hydrodynamic performance of a propeller in open water conditions. Thoroughly, the simulation utilizes the Computational Fluid Dynamics (CFD) approach, implementing the Reynolds-Averaged Navier-Stokes (RANS) equations to capture and analyze hydrodynamic interactions around the propeller blade. In other words, the results provided a comprehensive elucidation of the hydrodynamic characteristics underlying the findings. The computational simulations have taken into consideration various parameters, including the effects of propeller rotation speeds (RPM), blade numbers (Z), and pitch ratios (P/D) across a range of advanced ratios (J) from 0 to 1.0. The results, involving thrust coefficient, torque coefficient, and efficiency, reflective of the propeller's ability to convert rotational force into thrust, are comprehensively discussed in Section 4.

2. Theoretical Background

The theoretical background of propeller study encompasses key components like governing equations, turbulence models, and hydrodynamics theory. It provides a fundamental framework to understand propeller behaviour and performance, including fluid flow analysis, turbulent flow simulations, and calculation of important coefficients like thrust, torque, and efficiency.

2.1 Governing Equation

The continuity equation in fluid dynamics highlights constant mass. Computational fluid dynamics software uses the conservation of mass equation (Eq. (1)). It relates the rate of change of mass within a control volume to net inflow minus outflow and the rate of mass generation.

$$\frac{\delta \rho}{\delta t} + \nabla(\rho U) = G \tag{1}$$

Using finite volume methods, numerical solutions of the equation preserve mass throughout the simulation domain, ensuring accurate and reliable simulations by maintaining constant fluid mass and realistic behaviour over time.

The Navier-Stokes equations govern momentum conservation, relating forces, acceleration, and fluid behaviour (Eq. (2)). Numerical methods, like finite volume or finite element, solve these equations to calculate fluid velocity and pressure fields.

$$\frac{\delta(\rho v)}{\delta t} + \nabla(\rho u U) = -\nabla \mathrm{p} + \nabla \cdot \tau + \rho \mathrm{g} \quad (2)$$

By applying the law of momentum conservation, the software analyses and predicts fluid flow patterns, forces, and velocities. This ensures accurate simulations and predictions in fluid dynamics.

2.2 Turbulence Model

The Spalart-Allmaras model is utilized in this study as a turbulence model for turbulent flow simulation. It is based on the Reynolds-averaged Navier-Stokes equations and employs a single transport equation for the eddy viscosity (v_t). The governing equation of the Spalart-Allmaras model is shown in Eq. (3).

$$\frac{\partial \tilde{v}}{\partial t} + u \cdot \nabla \tilde{v} = c_{b1} S \tilde{v} - c_{w1} f_w \left(\frac{\tilde{v}}{d}\right)^2 + \nabla \cdot [(v + \sigma \tilde{v}) \nabla \tilde{v}] + \frac{1}{\sigma} \cdot \nabla \tilde{v} \cdot \nabla \tilde{v} \quad (3)$$

The Spalart-Allmaras model excels in handling adverse pressure gradients and streamline curvature in boundary layers [5]. It predicts separated flows accurately and is computationally efficient.

2.3 Hydrodynamics Theory of Propeller

The propeller model was tested in open water conditions to assess its performance without ship resistance. To illustrate the evaluation results against the advance ratio (J), non-dimensional values like thrust (K_T), torque (K_Q), and efficiency (η) coefficients were computed using Eq. (4) based on water advance velocity:

$$J = \frac{v_a}{nD} \quad (4)$$

$$\eta = \frac{J}{2\pi} \frac{K_T}{K_Q} \quad (5)$$

$$K_T = \frac{T}{\rho n^2 D^4} \quad (6)$$

$$K_Q = \frac{Q}{\rho n^2 D^5} \quad (7)$$

Eq. (5) demonstrates that propeller efficiency relies on crucial input values derived from Eq. (6) and (7).

3. Simulation Condition

Referring to the main objective, the CFD simulation scrutinizes propeller performance in open-water conditions. This investigation thoroughly elaborates on simulation conditions, encompassing

propeller properties, parametric studies, computational domain, meticulous mesh generation, and a comprehensive exploration of mesh independence.

3.1 Principal Data of Propeller

Here, the propeller data provided by PT. Terafulk Megantara Design as the actual design propeller specifications. Displaying the principal dimensions of the left-handed propeller, the data in Table 1 presents geometric factors, including diameter, pitch, chord length, and blade area. This data designates both full-scale and model-scale propellers (scaled at 1:30.6). For a clearer insight, refer to Figure 1, where the precise 3D model visually presents the accurate main dimensions of the propeller.

Table 1
Main dimensions of propeller

Geometrical parameters	Full Scale	Model Scale
Diameter (mm)	3650	119.25
AE/AO	0.695	0.695
P/D	1.013	1.013
Pitch (mm)	3697.45	120.83
Scale	1:30.6	
Orientation	Left-Handed Rotation	

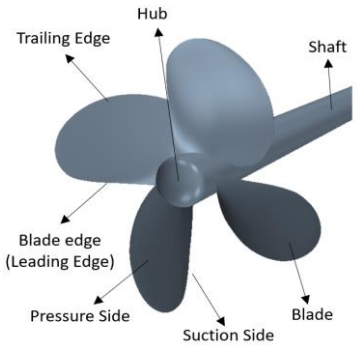

Fig. 1. Geometry of propeller

3.2 Parametric Studies

The present CFD simulation analyses the impact of propeller revolutions, blade numbers, and pitch ratios on performance. Tables 2 and 3 summarize the conditions. The study aims to understand how these parameters affect propeller behaviour.

Table 2
Matrix of simulations at various RPM and blade numbers conditions

P/D	Propeller Revolution (RPM)			Z
	1100	1200	1300	
1.2	O	√	O	3
	√	√	√	4
	O	√	O	5

Table 3
Matrix of simulations at various pitch ratio conditions

RPM	Pitch Propeller (P/D)			
	0.6	0.8	1.0	1.2

1200	√	√	√	√

3.3 Computational Domain and Meshing Generation

The computational domain consists of two regions: the rotational region (Figure 2 and Table 4) containing the propeller as the rotating body, and the static region encompassing the Inlet, Outlet, and Far Field. Figure 2 displays the boundary conditions for each face. Assigning blade edges accurately captures the propeller's shape, focusing on the thinnest part of the blades where they first interact with the water.

Table 4
Boundary conditions

Faces	Condition	Input Value
Inlet	Velocity Inlet	0.0 – 1.0 m/s
Outlet	Pressure Outlet	14729.72 Pa
Far Field	Symmetry Plane	-
Interfaces	Symmetry Plane	-
Propeller	Wall	No Slip

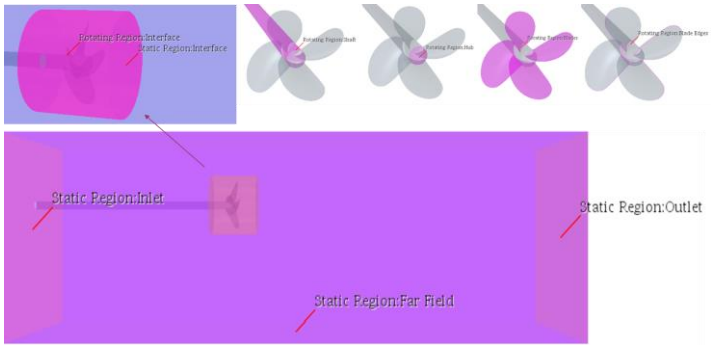

Fig. 2. Boundary condition of static and rotating regions

3.4 Mesh Independence Study

A mesh independence study investigated the optimal number of mesh cells for accurate results [6]. Table 5 presents the results, with four cases spanning a total mesh cell count range of 0.5 to 3 million. The objective was to identify a mesh size that balances result sensitivity, reliability, and computational efficiency.

Table 5
Mesh independence study

Case	Total Mesh Number	J	K_T	K_Q	η
A	0.5 million	0.3	0.3959	0.4910	0.2885
B	1 million		0.3119	0.5022	0.2965
C	2 million		0.3361	0.5139	0.3121
D	3 million		0.3366	0.5154	0.3117

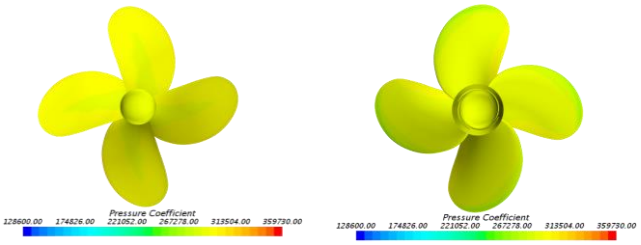

(a) (b)

Fig. 3. Visualization of pressure coefficient at (a) suction side and (b) pressure side

Among the tested cases, Case C was selected, showing a thrust coefficient of 0.3361, torque coefficient of 0.5139, and efficiency of 0.3121 at J = 0.3. It utilized 2.67 million mesh cells, providing accurate results with less computation time compared to Case D. This approach has been validated by Adam *et al.,* [7] and Fitriadhy *et al.,* [8].

Upon concluding the CFD simulation, Figure 3 exhibited the scalar torque and static pressure for various propeller configurations. The simulation was validated with an appropriate total mesh count, and Table 6 showed good agreement with the experimental model test.

Table 6
CFD and experimental results associated with Z=4 and RPM=1200

J	K_T			$10K_Q$			η		
	CFD	EXP	(%)	CFD	EXP	(%)	CFD	EXP	(%)
0.50	0.2554	0.2774	7.93	0.4121	0.4485	8.12	0.4929	0.4920	0.18

The percentage discrepancy error between experimental and CFD results for KT, KQ, and η was within an acceptable range of approximately 1.04%, 2.24%, and 1.23%, respectively, similar to Tan *et al.,* [9].

4. Results and Discussion

The section analyzed propeller performance under various RPM, Z, and P/D settings, presenting results for K_T, K_Q, and η values.

4.1 Effects of Various Propeller Revolution (RPM) on Propeller Performance

The CFD simulation analyzed the propeller's performance at varying rotational speeds (1100-1300 RPM) (refer to Figure 4). Higher speeds were associated with increased thrust and efficiency values. The propeller at 1100 RPM displayed the highest thrust coefficient, while at 1300 RPM, it exhibited the lowest. The pressure differences between the propeller blade sides contributed to this behavior, consistent with Fitriadhy *et al.,* [8] findings. As a result, the blades generated more lift leading to enhanced thrust. The highest efficiency occurred at J = 0.8 for 1100 RPM, where the blades experienced the lowest pressure compared to 1200 and 1300 RPM (refer to Table 7).

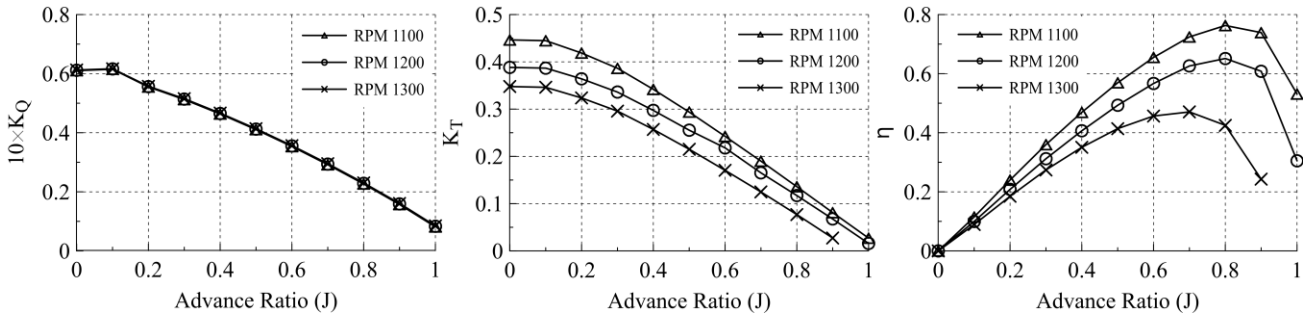

Fig. 4. $10K_Q$, K_T and η of the propeller at various propeller revolution versus advanced ratio for Z=4 and P/D = 1.0

Table 7
Torque, thrust and efficiency coefficients of propeller at various propeller revolutions

J	Propeller Revolution (RPM)								
	K_T			$10*K_Q$			η		
	1100	1200	1300	1100	1200	1300	1100	1200	1300
0.0	0.4464	0.3882	0.3477	0.6103	0.6113	0.6123	0	0	0
0.1	0.4448	0.3867	0.3461	0.6149	0.6160	0.6166	0.1150	0.0998	0.0893
0.2	0.4186	0.3640	0.3236	0.5550	0.5562	0.5573	0.2400	0.2082	0.1848
0.3	0.3864	0.3360	0.2958	0.5124	0.5139	0.5152	0.3599	0.3120	0.2741
0.4	0.3418	0.2972	0.257	0.4636	0.4651	0.4664	0.4691	0.4066	0.3507
0.5	0.2937	0.2554	0.2151	0.4105	0.4121	0.4135	0.5691	0.4929	0.4139
0.6	0.2424	0.218	0.1705	0.3534	0.3551	0.3565	0.6549	0.5667	0.4566
0.7	0.1899	0.1651	0.1248	0.2919	0.2937	0.2953	0.7244	0.6260	0.4705
0.8	0.1359	0.1172	0.0769	0.2268	0.2287	0.2303	0.7630	0.6513	0.4251
0.9	0.0811	0.0675	0.0273	0.1571	0.1591	0.1608	0.7389	0.6081	0.2429
1.0	0.0271	0.0159	-	0.0813	0.0833	0.085	0.5313	0.3050	-

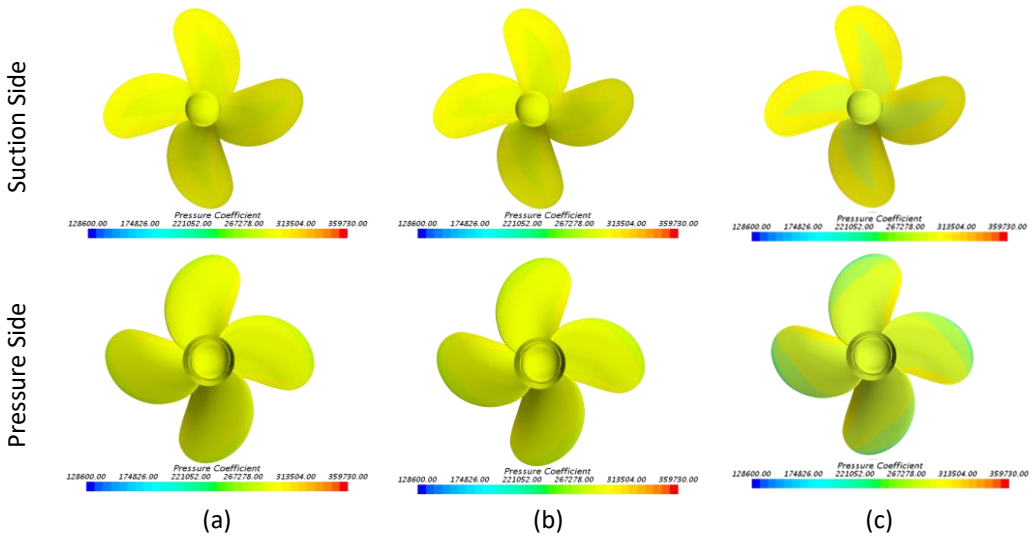

Fig. 5. Pressure coefficient for J = 0.5 at various propeller revolutions (a) 1100 RPM, (b) 1200 RPM, and (c) 1300 RPM

The propeller's suction and pressure sides behave differently at varying RPMs (refer to Figure 5). Lower RPMs cause smoother flow patterns on both sides due to reduced velocity, resulting in lower dynamic pressure on the suction side and a gentler deceleration on the pressure side. At 1300 RPM, the pressure side shows a larger green region than the 1100 RPM propeller. These flow patterns affect thrust generation and efficiency.

4.2 Effects of Various Number Of Blades (Z) on Propeller Performance

Referring to Figure 6, the effect of blade number (Z) on propeller performance had been investigated where three different blade numbers, Z = 3, 4, and 5, had been used in this analysis. The results were presented as a comparison of thrust coefficient, torque coefficient, and efficiency. It had been observed that propellers with 5 blades had the highest thrust and torque coefficients, while the propeller with 3 blades number at J=0.8 had exhibited the highest efficiency. This finding had aligned with the study conducted by Fitriadhy *et al.,* [10]. This was due to the increasing number of blades having led to a greater contact area with the water flow, resulting in increased water drag force and higher power consumption to overcome it [11]. Additionally, a higher blade number had increased turbulence, which had disrupted the water flow between neighboring blades and had reduced the effective thrust delivery. Propellers with more blades had generated more thrust and torque (refer Table 8), they had also experienced higher total pressure and had exhibited lower efficiency.

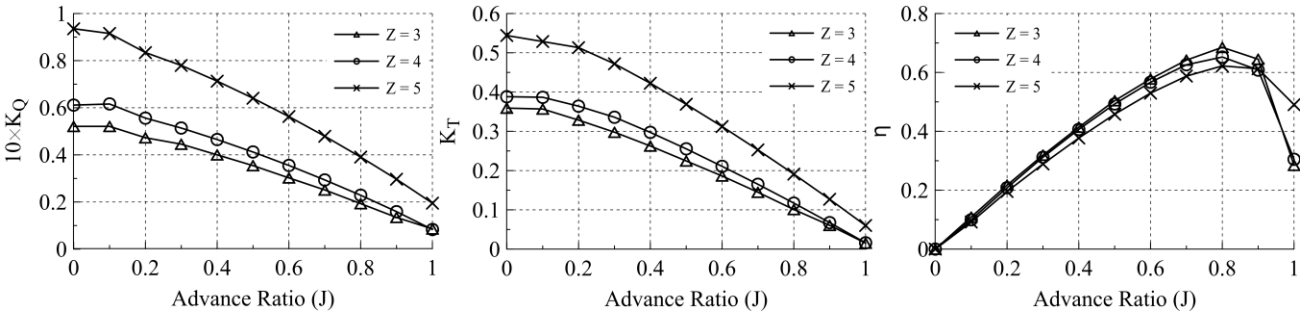

Fig. 6. $10K_Q$, K_T and η of the propeller at various blade numbers versus advanced ratio for RPM = 1200 and P/D = 1.0

Table 8
Torque, thrust and efficiency coefficients of propeller at various blade numbers

J	Blades Number (Z)								
	K_T			$10*K_Q$			η		
	Z = 3	Z = 4	Z = 5	Z = 3	Z = 4	Z = 5	Z = 3	Z = 4	Z = 5
0.0	0.3591	0.3882	0.5440	0.5209	0.6113	0.9355	0	0	0
0.1	0.3568	0.3867	0.5286	0.5209	0.6160	0.9153	0.1089	0.0998	0.0918
0.2	0.3285	0.3640	0.5132	0.4728	0.5562	0.8344	0.2173	0.2082	0.1956
0.3	0.2978	0.3360	0.4720	0.4455	0.5139	0.7795	0.3190	0.3120	0.2890
0.4	0.2626	0.2972	0.4225	0.4001	0.4651	0.7130	0.4140	0.4066	0.3771
0.5	0.2245	0.2554	0.3689	0.3544	0.4121	0.6405	0.5040	0.4929	0.4581
0.6	0.1863	0.2108	0.3122	0.3023	0.3551	0.5626	0.5779	0.5667	0.5297
0.7	0.1448	0.1651	0.2527	0.2512	0.2937	0.4792	0.6418	0.6260	0.5874
0.8	0.1009	0.1172	0.1910	0.1932	0.2287	0.3908	0.6852	0.6523	0.6222
0.9	0.0605	0.0675	0.1269	0.1345	0.1591	0.2967	0.6448	0.6081	0.6124
1.0	0.0153	0.0159	0.0601	0.0859	0.0833	0.1951	0.2846	0.3050	0.4905

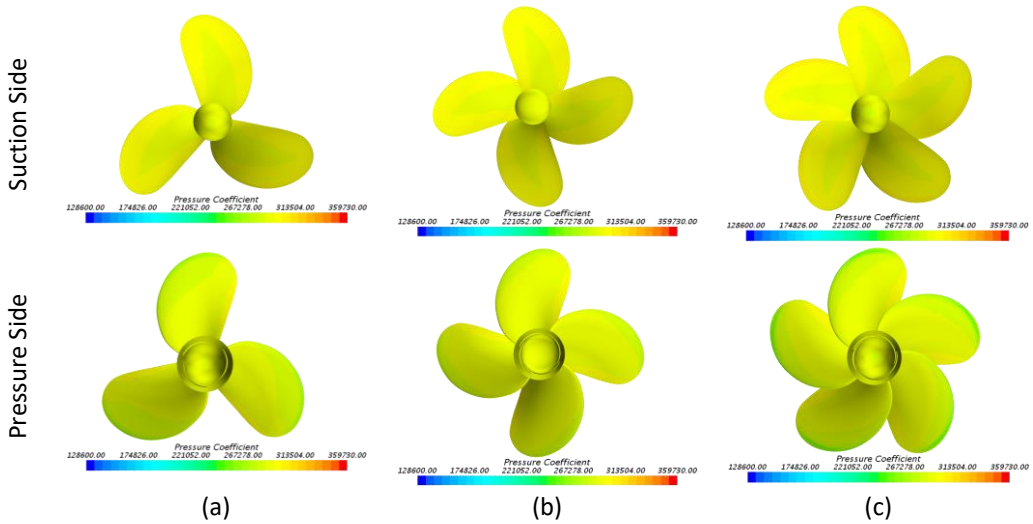

Fig. 7. Pressure coefficient for J = 0.5 at various blade numbers (a) Z = 3, (b) Z = 4, and (c) Z = 5

The pressure distribution on the suction and pressure sides of the propeller blades varied with different blade numbers. Increasing blade numbers caused reduced pressure near the leading edge on the suction side due to a greater suction effect, while on the pressure side, it led to increased pressure due to fluid compression from the increased blade area. Figure 7 illustrates how blade number influences pressure distribution on both sides of the propeller blades. This finding highlights the significance of blade numbers in determining pressure distribution and flow behavior in propellers, with implications for design and performance.

4.3 Effects of Various Pitch Ratios (P/D) on Propeller Performance

The study investigated propellers with varying pitch ratios (P/D = 0.6 to 1.2) and their performance in thrust coefficient, torque coefficient, and efficiency. Increasing the pitch ratio improved the torque coefficient, as shown in Figure 8. Propellers with P/D = 1.2 consistently outperformed the thrust coefficient, while P/D = 0.6 had the lowest efficiency. These findings were consistent with Andou and Addulkareem's [12] study, attributing it to a higher pitch ratio pushing more water astern, generating more torque but reducing thrust coefficient due to the effective angle of attack decrease. Table 9 confirmed the highest pitch ratio produced more torque but decreased thrust efficiency. In summary, propeller performance was influenced by pitch ratio, affecting thrust and torque differently [12].

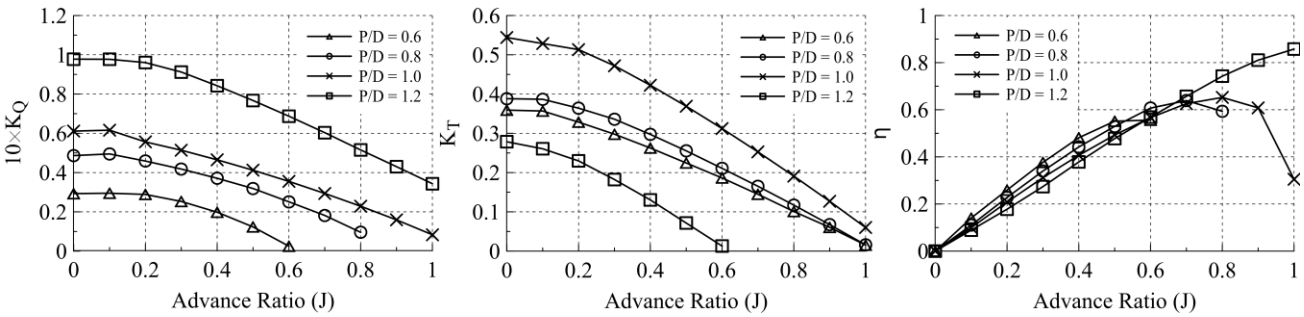

Fig. 8. $10K_Q$, K_T and η of the propeller at various pitch ratios versus advanced ratio for RPM = 1200 and Z = 4

Table 9
Torque, thrust and efficiency coefficients of propeller at various pitch ratios

J	Pitch ratio (P/D)											
	K_T				$10*K_Q$				η			
	0.6	0.8	1.0	1.2	0.6	0.8	1.0	1.2	0.6	0.8	1.0	1.2
0.0	0.2785	0.3324	0.3882	0.5531	0.2930	0.4865	0.6113	0.9777	0	0	0	0
0.1	0.2606	0.3434	0.3867	0.5473	0.2950	0.4950	0.6160	0.9771	0.1405	0.1103	0.0998	0.0891
0.2	0.2297	0.3284	0.3640	0.5370	0.2888	0.4587	0.5562	0.9603	0.2593	0.2278	0.2082	0.1779
0.3	0.1823	0.2977	0.3360	0.5233	0.2530	0.4180	0.5139	0.9121	0.3767	0.3399	0.3120	0.2738
0.4	0.1303	0.2577	0.2972	0.5009	0.1983	0.3710	0.4651	0.8423	0.4813	0.4420	0.4066	0.3784
0.5	0.0715	0.2123	0.2554	0.4606	0.1232	0.3189	0.4121	0.7671	0.5514	0.5295	0.4929	0.4776
0.6	0.0129	0.1597	0.2108	0.4093	0.0252	0.2511	0.3551	0.6872	0.5561	0.6071	0.5667	0.5686
0.7	-	0.1042	0.1651	0.3559	-	0.1817	0.2937	0.6033	-	0.6390	0.6260	0.6570
0.8	-	0.0447	0.1172	0.3006	-	0.0958	0.2287	0.5153	-	0.5933	0.6523	0.7424
0.9	-	-	0.0675	0.2435	-	-	0.1591	0.4302	-	-	0.6081	0.8106
1.0	-	-	0.0159	0.1851	-	-	0.0833	0.3434	-	-	0.3050	0.8576

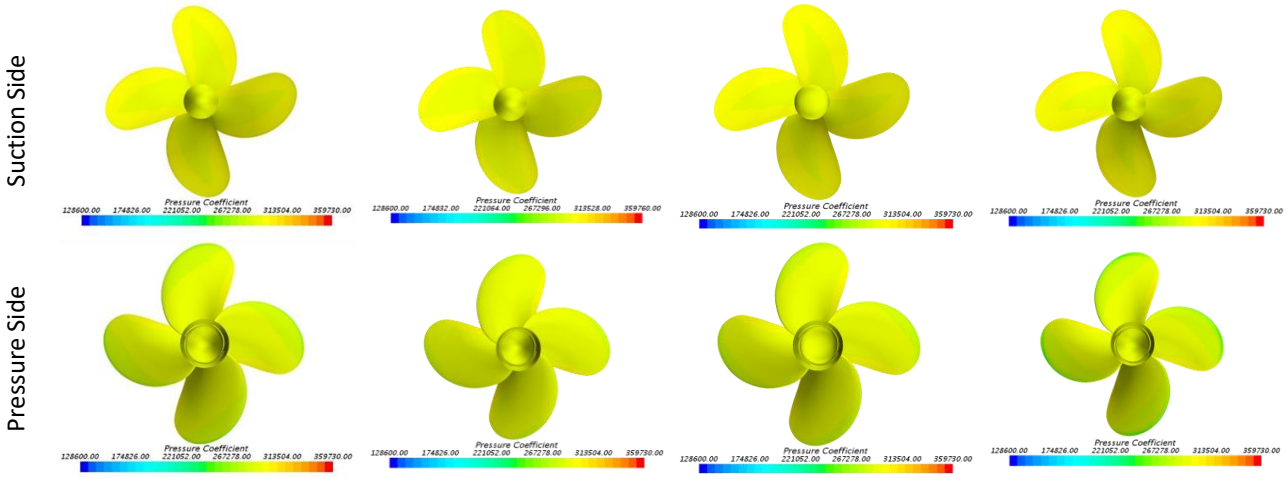

Fig. 9. Pressure coefficient for J = 0.5 at various pitch ratio (a) P/D = 0.6, (b) P/D = 0.8, (c) P/D = 1.0 and (d) P/D = 1.2

The performance of a propeller is significantly influenced by the pressure distribution on its blades. To investigate this, the study focused on the effects of various pitch ratios, particularly at the highest pitch ratio. Observations revealed distinct changes in pressure distribution on both the suction and pressure sides of the blades. This closely relates to the research carried out by Ren *et al.,* [13]. On the suction side, increasing the pitch ratio resulted in decreased pressure at low advance ratios due to higher water pressure at the leading edge. This led to a higher pressure drag force on the blades, contributing to increased torque production. On the pressure side, higher pitch ratios caused a decrease in pressure at the leading edge due to the higher axial velocity experienced. The higher axial velocity effectively reduced the pressure on the pressure side of the blades. When comparing pressure distribution among different pitch ratios, similarities were found by Abdou and A-Obaidi [14] and Cong *et al.,* [15]; where the blades with the highest pitch ratio experienced lower pressure levels compared to those with lower pitch ratios. This is evident in Figure 9 of the pressure distribution diagram, where a larger shaded green area highlights the highest pitch ratio propeller. Understanding these pressure distribution effects is crucial for comprehensively analyzing the propeller's performance.

5. Conclusions

The propeller performance in the open water conditions was successfully predicted using the CFD approach. The study investigated the effects of pitch ratios (P/D), rotational speeds (RPM), and blade numbers (Z). The findings are summarized as follows:

- A higher advance ratio caused decreased K_T and K_Q due to lower axial velocity and increased pressure drag at low J values. Propeller efficiency increased with J to an optimum value, then dropped significantly.
- Higher propeller RPMs decreased efficiency due to increased power requirements. Among tested speeds (1100 RPM, 1200 RPM, and 1300 RPM), 1100 RPM showed the highest efficiency.
- Adding more blades increased thrust and torque, but reduced efficiency due to increased pressure. Three blades (Z=3) demonstrated the best efficiency, while five blades (Z=5) showed higher thrust and torque.
- The pitch ratio positively affected the propeller's hydrodynamic performance, with higher ratios increasing thrust torque and efficiency. P/D=1.2 showed the highest efficiency at J=1.0.

In conclusion, Computational Fluid Dynamics (CFD) provided suitable preliminary propeller performance predictions. While the analysis achieved its objectives, further investigations are required to explore the effects of different propeller designs on hydrodynamic performance.

Acknowledgement
The authors wish to greatly thank for the PT. Terafulk Megantara Design for providing the propeller model.

References

[1] Ekinci, Serkan. "A practical approach for design of marine propellers with systematic propeller series." *Brodogradnja: Teorija i praksa brodogradnje i pomorske tehnike* 62, no. 2 (2011): 123-129.
[2] Tsujimoto, Masaru, Mariko Kuroda, Naoto Sogihara, and Akiko Sakurada. "Development of Empirical Formulae for Estimating Ship Performance." *National Maritime Research Institute* 18, no. 3 (2018): 91-106.
[3] Zou, Donglin, Jianghai Xu, Jing Zhang, Fangrui Lv, Na Ta, and Zhushi Rao. "The hydroelastic analysis of marine propellers considering the effect of the shaft: Theory and experiment." *Ocean Engineering* 221 (2021): 108547. https://doi.org/10.1016/j.oceaneng.2020.108547
[4] Ebrahimi, A., A. H. Razaghian, A. Tootian, and M. S. Seif. "An experimental investigation of hydrodynamic performance, cavitation, and noise of a normal skew B-series marine propeller in the cavitation tunnel." *Ocean Engineering* 238 (2021): 109739. https://doi.org/10.1016/j.oceaneng.2021.109739
[5] Li, Wenhao, and Yangwei Liu. "Study of limits to the rotation function in the SA-RC turbulence model." *Chinese Journal of Aeronautics* 36, no. 1 (2023): 246-265. https://doi.org/10.1016/j.cja.2022.05.015
[6] Seeni, Aravind, Parvathy Rajendran, and Hussin Mamat. "A CFD mesh independent solution technique for low Reynolds number propeller." (2021).
[7] Adam, N. Amira, A. Fitriadhy, C. J. Quah, and T. Haryanto. "Computational analysis on B-series propeller performance in open water." *Marine Systems & Ocean Technology* 15, no. 4 (2020): 299-307. https://doi.org/10.1007/s40868-020-00087-z
[8] Fitriadhy, Ahmad, Nur Amira Adam, C. J. Quah, Jaswar Koto, and Faisal Mahmuddin. "CFD prediction of b-series propeller performance in open water." *CFD letters* 12, no. 2 (2020): 58-68.
[9] Tan, Yue, Jing Li, Yuan Li, and Chunbao Liu. "Improved performance prediction of marine propeller: numerical investigation and experimental verification." *Mathematical Problems in Engineering* 2019 (2019). https://doi.org/10.1155/2019/7501524
[10] Fitriadhy, Ahmad, N. Amira Adam, and C. J. Quah. "Computational prediction of a propeller performance in open water condition." *Sinergi* 24, no. 2 (2020): 163-170. https://doi.org/10.22441/sinergi.2020.2.010

[11] Adeyeye, Kehinde Adeseye, Nelson Ijumba, and Jonathan Colton. "The Effect of the Number of Blades on the Efficiency of a Wind Turbine." In *IOP Conference Series: Earth and Environmental Science*, vol. 801, no. 1, p. 012020. IOP Publishing, 2021. https://doi.org/10.1088/1755-1315/801/1/012020
[12] Abdou, Mohamed, and Abdulkareem Sh Mahdi Al-Obaidi. "Studying the Effect of Pitch Ratio on Sheet Cavitation in Marine Propellers." *J. Eng. Sci. Technol* 13 (2018): 28-38.
[13] Ren, Zhen, Lin Hua, and Penghui Ji. "Numerical Analysis on Hydrodynamic Characteristics of Surface Piercing Propellers in Oblique Flow." *Water* 11, no. 10 (2019): 2015. https://doi.org/10.3390/w11102015
[14] Abdou, Mohamed, and Abdulkareem Sh Mahdi Al-Obaidi. "Studying the Effect of Pitch Ratio on Sheet Cavitation in Marine Propellers." *J. Eng. Sci. Technol* 13 (2018): 28-38.
[15] Cong, NGUYEN Chi, LUONG Ngoc Loi, and N. Van He. "A study on effects of blade pitch on the hydrodynamic performances of a propeller by using cfd." *Journal of Shipping and Ocean Engineering* 8 (2018): 36-42. https://doi.org/10.17265/2159-5879/2018.01.005